metals

MDPI

Article

Solidification Pattern of Si-Alloyed, Inoculated Ductile Cast Irons, Evaluated by Thermal Analysis

Iuliana Stan, Denisa Anca *, Stelian Stan and Iulian Riposan

Materials Science and Engineering Faculty, Politehnica University of Bucharest, 060042 Bucharest, Romania; iuliana.stan@upb.ro (I.S.); constantin.stan@upb.ro (S.S.); iulian.riposan@upb.ro (I.R.)
* Correspondence: denisa_elena.anca@upb.ro

Abstract: The solidification cooling curve itself as well as its first derivative, and related temperatures, reported to the calculated equilibrium temperatures in stable and metastable solidification systems, are used to predict the solidification characteristics of the cast iron. Silicon, as the most representative cast iron element, and inoculation, as graphitizing metallurgical treatment, have a major influence on the transition from the liquid to the solid state. Six experimental programs are performed, with Si content typically for non-alloyed (<3.0% Si), low (3.0–3.5% Si) and medium alloyed (4.5–5.5% Si) ductile cast irons, as Si-content increasing, and inoculation simultaneous effects. Silicon is an important influencing factor, but the base and minor elements also affect the equilibrium eutectic temperatures, much more in the Fe-C-Si-*Xi* stable system (15–20 °C) than in the metastable system (5–10 °C), comparing with their calculation based only on a Si effect (Fe-C-Si system). The highest positive effect of inoculation is visible in non-Si alloyed cast irons (2.5% Si): 9–15 °C for the eutectic reaction and 3 to 4 times increased at the end of solidification (37–47 °C). Increased Si content decreases inoculation power to 7–9 °C for low alloying grade (up to 3.5% Si), with the lowest contribution at more than 4.5% Si (0.3–2.0 °C). 2.5–3.5% Si ductile cast irons are more sensitive to high solidification undercooling, especially at the end of solidification (but with a higher efficiency of inoculation), compared to 4.5–5.5% Si ductile cast irons, at a lower undercooling level, and at lower inoculation contribution, as well.

Keywords: ductile cast iron; solidification; eutectic reaction; end of solidification; stable system; metastable system; cooling curve analysis; silicon alloying; inoculation; eutectic undercooling

Citation: Stan, I.; Anca, D.; Stan, S.; Riposan, I. Solidification Pattern of Si-Alloyed, Inoculated Ductile Cast Irons, Evaluated by Thermal Analysis. *Metals* **2021**, *11*, 846. https://doi.org/10.3390/met11050846

Academic Editor: Annalisa Fortini

Received: 20 April 2021
Accepted: 14 May 2021
Published: 20 May 2021

1. Introduction

By free carbides avoiding and ferrite promoting, silicon has an important contribution to reach high ductility and toughness characteristics, accompanied by the best machinability conditions. The presence of the silicon atoms inside the ferrite structure contributes to increasing the tensile strength *Rm* ((+128 MPa)/% Si—maximum reached at 4.2–4.4% Si), the yield strength $Rp_{0.2}$ ((+118 MPa)/% Si—maximum reached at 4.6–4.8% Si), and the Brinell hardness ((+45 HB)/% Si—for 2.5–6% Si (150 HB to 310 HB), but with a drastic decrease of elongation *A* ((−5% *A*)/% Si)—at less than 4.3% Si, and (−30% *A*)/% Si, for 4.3% up to 4.8% Si) of the ferritic ductile cast irons [1].

In 3.2–4.3% Si ductile cast irons, the unstable mixed ferrite-pearlite matrix is replaced with more predictable and controllable ferritic grades, at a reduced hardness variation (±4 HB), increased cutting tool life, and better mechanical properties (*Rm* = 450–650 MPa; $Rp_{0.2}$ = 350–500 MPa; *A* = 10–20%); these materials are usually used in the automotive industry. Silicon (4–6% Si), and Si-Mo (2.5–5.5% Si, and 0.2–2.0% Mo) alloyed ductile cast irons are characterized by a high resistance to oxidation and corrosion at high temperatures. Molybdenum addition favors superior mechanical properties, especially at high temperatures (*Rm* = 400–650 MPa; $Rp_{0.2}$ = 250–550 MPa; *A* = 3–12%), typically for exhausted applications [2–4].

Inoculation, an important metallurgical treatment, is applied to the liquid cast iron, usually after the Mg-treatment to forestall solidification at an excessive eutectic undercooling degree, favorable for carbides occurrence or/and undesired graphite morphologies. In this way, it is possible to obtain an as-cast structure without free carbides (promoters of bad machinability and brittleness) and with a high quality graphite shape (the best expected graphite morphology specifically for each cast iron type, at a lower size and a higher nodule count).

Inoculation is recorded by addition of 0.05–1.0 wt.% alloy (inoculant, FeSiAl*X*, where *X* = Ca, Ba, Sr, RE, etc.) in the tapped iron melt (1300–1500 °C). The main objective of this treatment is to promote active compounds (microns scale) in the iron melt, to act as active graphite nucleation sites, at a lower eutectic undercooling, by improving the existent nucleation sites or/and by promoting new nucleation sites.

Factors influencing inoculation efficiency mainly refer to charge materials (pig iron/steel scrap ratio, recarburizers, preconditioners), melting furnace thermal regime, base iron chemical composition (Si, Mn, S) and iron residuals (Al, Ti, O, N), inoculating elements, inoculant type, inoculation procedure, holding time, pouring procedure, and casting characteristics [5].

Thermal (cooling curve) analysis is usually used to evaluate the solidification pattern of ductile cast irons, in terms of the prediction of eutectic undercooling, important for free carbide formation sensitivity, different graphite morphologies occurrence and the end of solidification defects (inter-eutectic cells free carbides and micro-shrinkage).

Important events on the cooling curve (the lowest and the highest eutectic temperatures and the temperature on the end of solidification), and on its first derivative (maximum recalescence rate, the lowest level at the end of solidification, different graphitizing factors) offer important information on the solidification pattern of ductile iron castings. The referring of these events to the equilibrium temperatures in the stable and metastable Fe-C systems offers more data on the specifics of primary structure characteristics [6–8].

The main objective of the present paper is to evaluate by thermal (cooling curve) analysis the solidification pattern of ductile cast irons, non-Si alloyed (<3.0% Si), low (3.0–3.5% Si), and medium Si alloyed (4.5–5.5% Si), as silicon content increases, while inoculation application effects present simultaneously on the cooling curves events.

2. Materials and Methods

Six experimental programs are performed, for three groups of ductile cast irons, with silicon content typically for non-alloyed (2.4–2.6% Si), lower limit (3.15–3.45% Si, low alloying grade), and upper limit (4.5–5.5% Si, medium alloying grade) of High-Si ductile cast irons (two programs for each group) (Table 1, Figure 1).

More information on some experimental programs and previous reported results are available in our previous published papers: Program I [8], Program II [2], Program III [9], Program IV [10], and Program V [11]. New obtained data are added to selected data from these previous papers, in order to have a coherent evaluation of the simultaneous influence of silicon and inoculation, for the entire range of silicon content in non-and Si alloyed ductile cast irons for applications involving mechanical properties and oxidation resistance, such as for the automotive industry.

Charge materials include steel scrap, ductile iron returns, ferrosilicon and recarburizer, typically used for commercial ductile irons production. Experimental cast irons, obtained by electric melting (10 kg—coreless induction furnace, 8000 Hz frequency, graphite crucible, 1500–1550 °C superheating), are subjected to a nodularization treatment (Tundish-Cover technique, 1.5–2.5 wt.% FeSiCaMgRE treatment alloys), followed by a FeSi-based alloys inoculation (Ca, Ba, Ce, Al as active elements), ladle and in-mold inoculation.

Table 1. Experimental programs parameters.

Pr *	Si Content (%)	Mg-Treatment ** (Nodularization)	Inoculation (Graphitization)
I	2.48	2.0 wt.% FeSiCaMgRE Tundish Cover Ladle	0.5 wt.% Ca, Ce, S, O-FeSi Pouring Ladle
II	2.55	2.0 wt.% FeSiCaMgRE Tundish Cover Ladle	0.3 wt.% Ca, Ce, S, O-FeSi Pouring Ladle
III	3.15	2.0 wt.% FeSiCaMgRE Tundish Cover Ladle	0.5 wt.% Ca, Ba, Al-FeSi Pouring Ladle
IV	3.44	2.5 wt.% FeSiCaMgRE Tundish Cover Ladle	0.5 wt.% Ca, Ba, Al-FeSi Pouring Ladle
V	4.55	1.5 wt.% FeSiCaMgRE Tundish Cover Ladle	0.1 wt.% Ca, Ba, Al-FeSi In-mold, Quick-Cup^{TM}
VI	5.25	1.5 wt.% FeSiCaMgRE Tundish Cover Ladle	0.1 wt.% Ca, Ba, Al-FeSi In-mold, Quick-Cup^{TM}

* Pr—Experimental Program; ** RE—Rare Earth Elements.

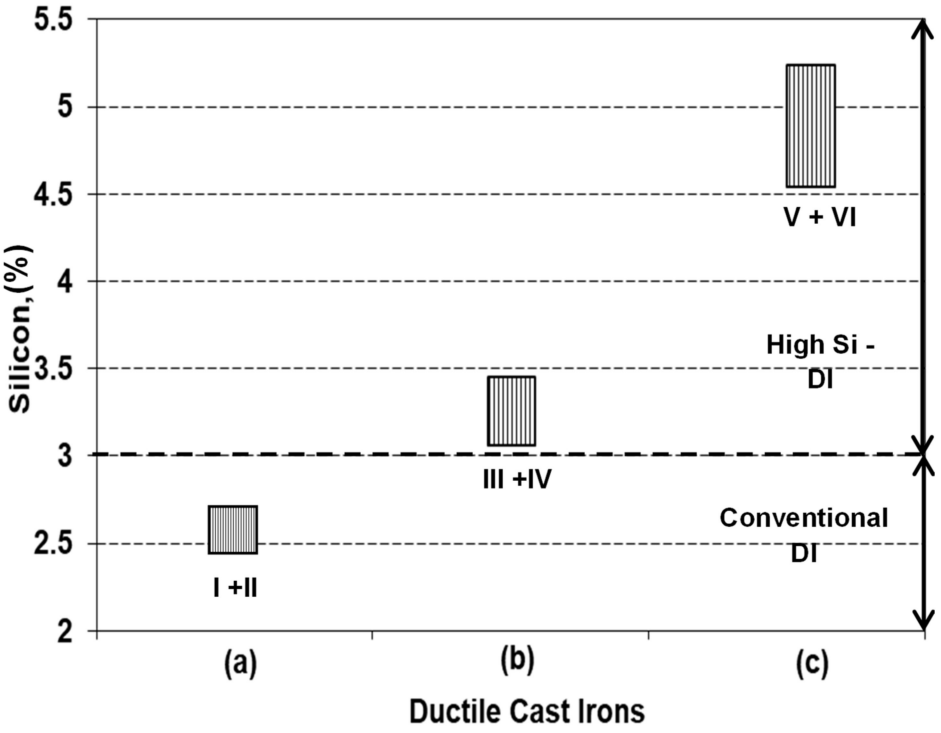

Figure 1. Representative groups of experimental programs (Table 1) (**a**) non-Si alloyed; (**b**) low-Si alloyed; (**c**) medium-Si alloyed).

Mg-treatment alloys include 43–46% Si, 6–10% Mg, 1–2% Ca, 0.8–1.5% Al, Fe-bal. Ca, Ba, Al-FeSi alloys (0.94–1.0% Ca, 1.0–1.68% Ba, 0.96–1.1% Al, 72.6–75% Si, Fe-bal) and Ca, Ce, S, O-FeSi alloys (70–76% Si, 0.75–1.25% Ca, 0.75–1.25% Al, 1.5–2.0% RE, and less than O and S-bearing compounds) [5] are selected as inoculants.

In ductile iron production, both the ladle and in-mold inoculation techniques are used. For higher silicon content ductile cast irons (>4% Si), trials V and VI, inoculation was recorded just in the ceramic cup, and used for thermal (cooling curve) analysis, as this inoculation technique is known to have the highest efficiency. This is considered necessary for high Si content ductile irons, according to the previously obtained results [2].

A SPECTROLAB high-end spectrometer (SPECTROLAB, Sylmar, CA, USA) with hybrid optic (photomultiplier tubs (PMT) and CCD (Spectroscopic Charge Coupled Device detection system) detectors simultaneously are used for high precision metal analysis. The instrument achieves detection limits below 1 mg/kg.

The present paper focuses on the thermal (cooling curve) analysis (standard Quick-Cup^{TM} (Heraeus Electro-Nite International, Houthalen, Belgium) thermal analysis) [12] of the Mg-treated liquid cast irons, before and after the inoculation process. Un-inoculated and inoculated iron melts are poured in standard ceramic cups (7.3 mm cooling modulus), including a thermocouple for thermal (cooling curve) analysis of the solidification process. Cooling modulus is the ratio between the volume and the total surface area of castings; it expresses the capacity to transfer the heat from casting through the mold media, outwardly. A lower cooling modulus value leads to a higher solidification cooling rate, with important effects on the eutectic and eutectoid structure formation and characteristics.

3. Results and Discussion

3.1. Chemical Composition

Base (C, Si, Mn, P, S), nodularizing (Mg, Ce, La), inoculating (Ca, Al, Zr) and minor (Ti, As, Sn, Sb, Pb, Bi, V, Cu, Ni, Cr, Co, Mo, Nb, W) elements, usually present in the commercial cast irons are analyzed (Tables 2 and 3).

Table 2. Base chemical composition and chemistry control factors.

Pr *	Chemical Composition (wt.%)							Chemistry Control Factors		
	C	Si	Mn	P	S	Al	Mg	*CE* ** (%)	*K* ***	*Px* ****
I	3.32	2.48	0.50	0.04	0.011	0.014	0.045	4.11	0.89	2.35
II	3.20	2.55	0.38	0.013	0.015	0.014	0.032	4.03	0.90	1.94
III	3.65	3.15	0.10	0.013	0.004	0.002	0.049	4.60	1.38	0.47
IV	3.37	3.44	0.44	0.05	0.020	0.015	0.032	4.43	0.87	0.23
V	3.33	4.55	0.22	0.04	0.012	0.0054	0.035	4.65	1.59	1.72
VI	3.46	5.25	0.22	0.04	0.010	0.0065	0.045	5.05	1.66	1.52

* Pr—Experimental Program, ** *CE*—Equation (1); *** *K*—Equation (2); **** *Px*—Equation (3).

Table 3. Minor elements.

Pr *	Chemical Composition ** (wt.%)										
	Ti	As	Sn	Sb	Pb	Bi	V	Cu	Ni	Cr	Mo
I	0.013	0.003	0.004	0.001	0.0002	0.002	0.004	0.055	0.044	0.048	0.010
II	0.013	0.003	0.005	0.0009	0.0002	0.002	0.005	0.06	0.040	0.050	0.020
III	0.005	0.005	0.005	0.005	0.002	0.002	0.016	0.02	0.072	0.080	0.050
IV	0.0063	0.006	0.005	0.0015	0.0002	0.002	0.004	0.067	0.050	0.078	0.010
V	0.0067	0.019	0.015	0.040	0.003	0.001	0.008	0.17	0.10	0.050	0.070
VI	0.0073	0.020	0.013	0.019	0.004	0.0009	0.011	0.11	0.064	0.094	0.042

* Pr—Experimental Program, ** Other elements (wt.%): 0.004–0.015 Co, 0.002–0.006 Nb, 0.0002–0.008 W, 0.01–0.025 Zr, 0.0004–0.018 Ce, 0.0001–0.006 La, 0.004–0.016 Ca.

As chemistry control factors, carbon equivalent (*CE*, Equation (1)), antinodularizing factor (*K*, Equation (2)) [13] and pearlite promoting factor (*Px*, Equation (3)) [13] are considered.

$$CE = \%\ C + 0.3(\%\ Si + \%\ P) + 0.4(\%\ S) - 0.027(\%\ Mn) \quad (1)$$

$$K = 4.4(\%\ Ti) + 2.0(\%\ As) + 2.4(\%\ Sn) + 5.0(\%\ Sb) + 290(\%\ Pb) + 370(\%\ Bi) + 1.6(\%\ Al) \quad (2)$$

$$Px = 3(\%\ \mathrm{Mn}) - 2.65(\%\ \mathrm{Si} - 2) + 7.75(\%\ \mathrm{Cu}) + 90(\%\ \mathrm{Sn}) + 357(\%\ \mathrm{Pb}) + 333(\%\ \mathrm{Bi}) + 20.1(\%\ \mathrm{As}) + 9.60\ (\%\ \mathrm{Cr}) + 71.7(\%\ \mathrm{Sb}) \quad (3)$$

For 2.48–5.25% Si and 3.20–3.65% C, the experimental cast irons are characterized by a large range carbon equivalent *CE* = 4.03–5.05%: slightly hypo-eutectic position for conventional, non-Si alloyed cast irons (2.48–2.55% Si, 4.03–4.11% *CE*), hyper-eutectic position (*CE* = 4.43–4.60%) for a lower limit Si-alloyed cast irons (3.15–3.45% Si) and a strong hyper-eutectic behavior (*CE* = 4.65–5.05%) for the upper limit of Si-alloying ductile cast irons (4.55–5.25% Si). A residual magnesium level is typical for ductile cast irons (0.032–0.045% Mg_{res}), with a supplementary nodularization contribution of 0.0004–0.018% Ce_{res} and 0.0001–0.006% La_{res}.

Minor elements presence and content are typical for medium quality commercial ductile cast irons, characterized by an upper limit of antinodularizing factor *K*, Equation (2) (0.87–1.66). Equation (2) illustrates the influence and establishes a rank of some important elements, starting with aluminum (having the lowest detrimental effect), followed by tin and arsenic, titanium and antimony, up to the most hazardous elements, lead and bismuth. According to Thielman, in magnesium-treated irons, the complex antinodularizing factor *K* should not exceed 1.0 [13]. The presence of rare earth elements (Ce, La) in the final chemical composition is quite useful to counteract the negative effect of antinodularizing elements, as the *K* factor exceeds the 1.0 level [5].

Pearlite promoting factor *Px* (Equation (3)) is normally decreased by silicon content increasing, but it is increased by Mn and many minor elements, which could decrease or just counteract the silicon effect. According to the data in Tables 2 and 3, at the normal content of silicon (2.5% Si), cast irons are characterized by *Px* = 1.94–2.35, typically for ferritic-pearlitic cast irons. Higher silicon content for the second group (3.15–3.44% Si) and a lower level of minor elements leads to very low *Px* values (0.23–0.47), favorable for the ferritic structure. Despite the highest content of silicon (4.55–5.25% Si), the third group is characterized by an intermediate *Px* level (1.52–1.72), due to the higher incidence of presence of the minor elements. Then it could be concluded that the favorable effect of high silicon content in ferrite formation allows the tolerance of higher amounts of pearlite and carbide stabilizing elements in the chemical composition of the High-Si ductile cast irons [1,2,14,15].

3.2. Thermal (Cooling Curve) Analysis

The well-known Fe-C phase diagram is obtained in equilibrium conditions, with very pure materials, without minor elements, under vacuum melting and at very slow cooling rate (0.5–2.5 °C/min or 0.008–0.04 °C/s). On the contrary, the commercial cast irons solidified in non-equilibrium conditions in the foundry industry, as a result of the complex chemistry (usually more than 30 elements, see Tables 2 and 3), involving different charge materials and industrial melting procedures, with more than ten times higher castings solidification rate (>0.4 °C/s) [5,16].

As a result, the solidification process will be more complicated, strongly influenced by the cast iron chemical composition, characteristics of charge materials, melting parameters, metallurgical treatment applied to the molten iron, pouring parameters, castings characteristics, mold and core media, etc. Generally, the real Fe-C phase diagram is modified, in terms of representative temperatures and carbon concentration, while the solidification process is performed at a higher undercooling. Representative in this respect is the solidification cooling curve. A typical system of cooling curves [$T = f(t)$] and its first derivative [$dT/dt = f(t)$] is presented in Figure 2, referring to the Program I, Table 1.

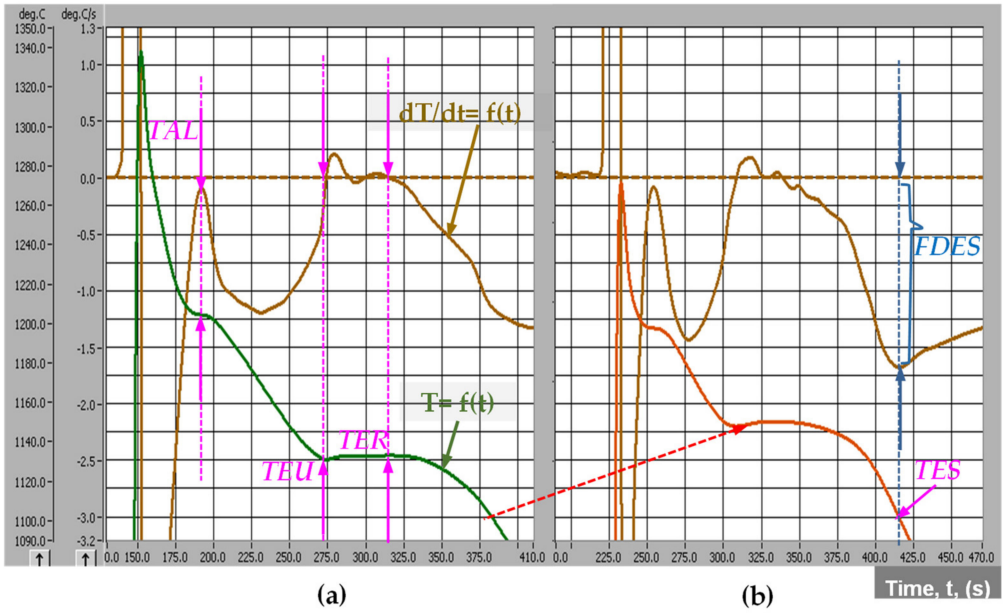

Figure 2. Typical cooling curves [T = f(t)] and their first derivative [dT/dt = f(t)] of un-inoculated (**a**) and inoculated (**b**) ductile cast irons (Program I, Table 1, *CE* = 4.11%) (*TAL*—temperature of austenitic liquidus; *TEU*—the lowest and *TER*—the highest eutectic temperatures; *TES*—temperature at the end of solidification; FDES—the lowest peak on the first derivative at the end of solidification).

The starting formation of the solid phase, as primary austenite, is clear marked by *TAL* (temperature of the austenitic liquidus) (Figure 2a), as a result of the heat released during austenite formation. It is corresponding to the zero level on the first derivative curve, and according to the hypo-eutectic position of this cast iron (*CE* = 4.11%). For hyper-eutectic cast irons, the primary graphite will be the first formed solid phase, corresponding to the *TGL*-temperature of the graphitic liquidus, usually less obvious on the cooling curve, due to the lower heat released during the graphite formation, comparing to the austenite.

TEU represents the lowest and *TER* the highest eutectic temperature on the cooling curve, both of them corresponding to zero level on the first derivative of the cooling curve (Figure 2a). Solid eutectic (austenite + graphite) formation means heat release, which could compensate for the lost heat; this process is usually expressed by a limited increasing temperature (from *TEU* up to *TER*), representing the eutectic recalescence. The temperature of the end of solidification (*TES*) corresponds to the lowest position of the first derivative at the end of solidification, *FDES* (Figure 2b).

Important information on the primary structure, especially expressed by carbides to graphite transition in the first part of eutectic reaction and on the results of the solidification of the last liquid iron in the areas between the eutectic cells (carbides, micro-shrinkage) could be obtained. This is possible if *TEU*, *TER* and *TES* parameters are reported to the eutectic equilibrium temperatures in graphitic (stable—T_{st}) and carbidic (metastable—T_{mst}) Fe-C systems. These temperatures have fixed values in the binary Fe-C system, but variable levels, depending on the presence, the content and the specific influence factor of other elements, which affect the carbon solubility in the liquid iron (Figure 3).

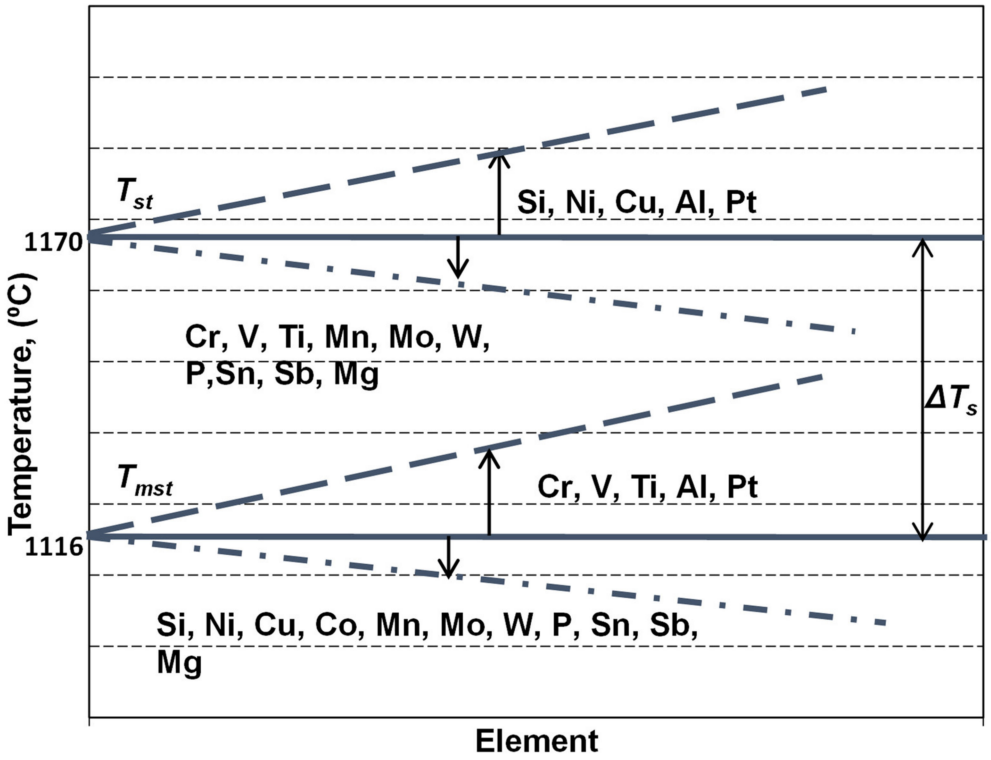

Figure 3. The influence of the chemical composition on the stable (T_{st}) and metastable (T_{mst}) eutectic temperatures in cast irons, as for the Fe-C-Si-*Xi* system alloys.

The simplest approach of a commercial cast iron is in a ternary system, as in the Fe-C-Si alloy, with silicon as an important influencing factor for T_{st} and T_{mst} evaluation, according to Equations (4) and (5) [17]. However, as the more realistic approach of a commercial cast iron is in the Fe-C-Si-*Xi* system, more complex equations, including the most important influencing elements in the chemical composition of commercial ductile cast irons are necessary, such as expressed by Equations (6) and (7) [18,19].

Recently [8] it was found that it is possible to have different values for T_{st} and T_{mst}, for a defined value of the silicon content. For this reason, T_{st} and T_{mst} parameters were calculated for both Fe-C-Si and Fe-C-Si-*Xi* systems, using the chemical composition included in Tables 2 and 3, by considering only silicon (S-series) and the full chemistry of the experimental cast irons (K-series) (Table 4, Figure 4).

Table 4. Calculated equilibrium eutectic temperatures T_{st} and T_{mst}.

Pr *	Si (%)	T_{st} (°C)		T_{mst} (°C)		$\Delta T_s = T_{st} - T_{mst}$ (°C)		ΔT_{st} (°C) (S–K)	ΔT_{mst} (°C) (S–K)
		S **	K ***	S	K	S	K		
I	2.48	1169.60	1151.80	1117.20	1106.60	52.40	45.20	17.80	10.60
II	2.55	1170.09	1153.40	1116.40	1106.70	53.69	46.70	17.55	9.70
III	3.15	1174.11	1161.03	1109.20	1105.01	64.91	56.02	13.08	4.19
IV	3.44	1176.05	1160.71	1105.72	1100.15	70.33	60.56	15.34	5.57
V	4.55	1183.49	1165.72	1092.40	1086.21	91.09	79.51	17.77	6.19
VI	5.25	1188.18	1169.17	1084.00	1079.11	104.18	90.06	19.01	4.89

* Pr—Experimental Program, ** *S*—Equations (4) and (5); *** *K*—Equations (6) and (7).

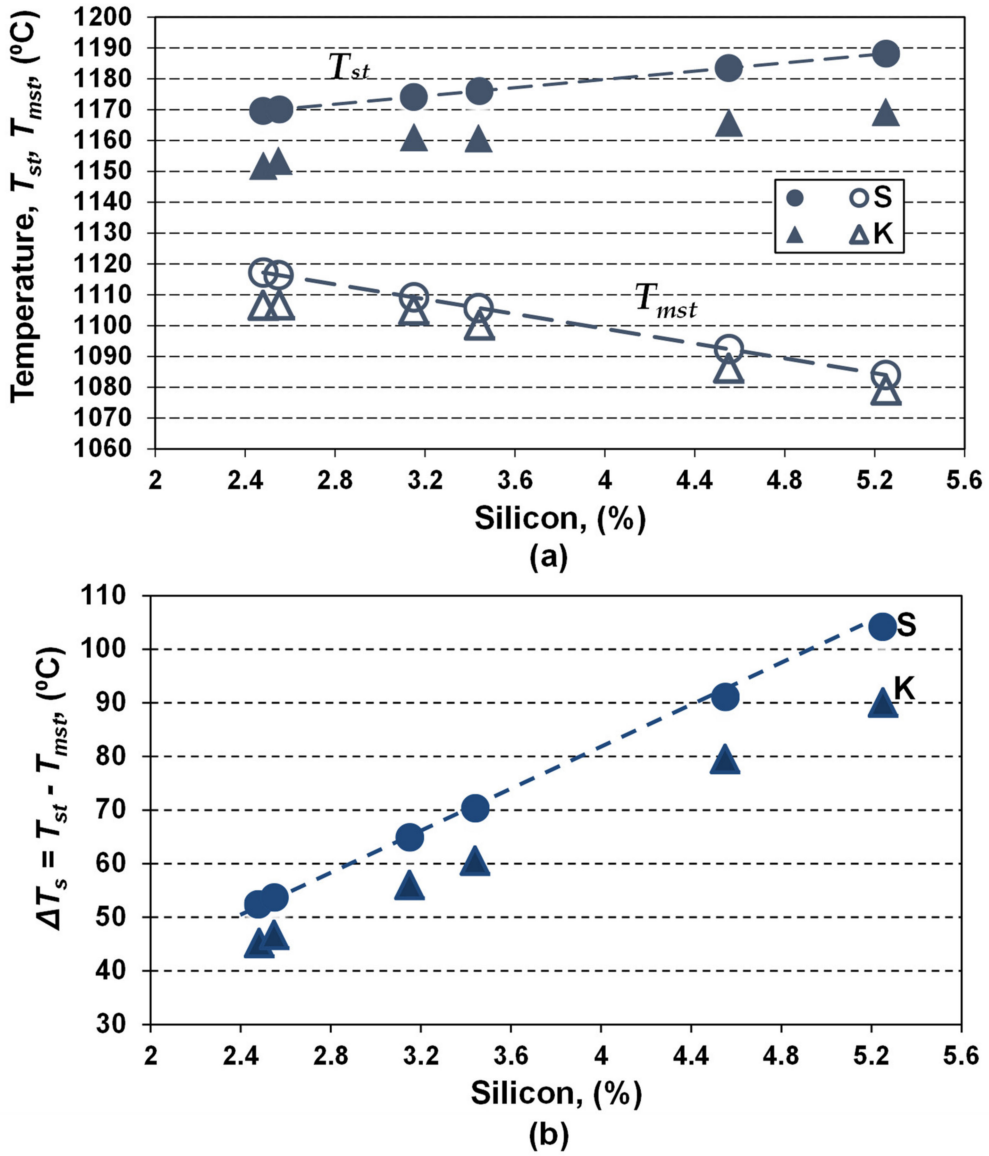

Figure 4. Influence of Si content on the T_{st} and T_{mst} eutectic temperatures (**a**) and the eutectic interval ΔT_s (**b**), for only Si effect (series S, Equations (4) and (5)) and complex chemical composition (series K, Equations (6) and (7)).

Silicon appears to have the most important effect, leading to the increasing of T_{st} and decreasing of T_{st} temperatures, and, consequently, enlarging the T_{st}–T_{mst} (ΔT_s) interval two times, as silicon increased from 2.5% up to 5.25% (series S).

For the real chemistry (series K), characterized by a multitude of elements, silicon remains the main influencing factor, but the results are affected by the presence of other elements.

$$T_{st} = 1153\ (^{\circ}C) + 6.7\ (\%\ Si) \quad (4)$$

$$T_{mst} = 1147\ (^{\circ}C) - 12\ (\%\ Si) \quad (5)$$

$$T_{st[TEG]} = 1149.1\ (^{\circ}C) + 4.7\ (\%\ Si) - 4.0\ [\%Sol.\ Mn] - 44\ (\%\ P) + 2.7\ (\%\ Cu) + 1.0\ (\%\ Ni) + 1.8\ (\%\ Co) + 13.9\ (\%\ Al) - 17.7\ (\%\ Mo) - 10.5\ (\%\ Cr) - 9.3\ (\%\ Sn) - 5.2\ (\%\ Sb) - 6.1\ (\%\ W) - 3.7\ (\%\ Nb) - 14.8\ (\%\ V) - 80.3\ (\%\ B) \quad (6)$$

$$T_{mst[TEC]} = 1142.6\ (^{\circ}C) - 11.6\ (\%\ Si) - 0.75\ [\%\ Sol.\ Mn] - 46.2\ (\%\ P) - 1.4\ (\%\ Cu) - 1.1\ (\%\ Ni) - 0.7\ (\%\ Co) - 1.8\ (\%\ Al) - 14.5\ (\%\ Mo) + 5.9\%\ Cr) - 6.0\ (\%\ Sn) - 5.1\ (\%\ Sb) - 2.8\ (\%\ W) + 0\ (\%\ Nb) + 3.3\ (\%\ V) - 26.0\ (\%\ B) \quad (7)$$

The base and minor elements affect the equilibrium eutectic temperatures, much more in the Fe-C-Si-*Xi* stable system (T_{st}, 15–20 °C) than in the metastable system (T_{mst}, 5–10 °C), comparing with their calculation as only the Si effect (Fe-C-Si), where the highest values resulted. It is found that if the pearlite formation potential is higher, as effects of Mn and some minor elements (Cu, Sn, Pb, Bi, As, Cr, Sb), the higher is the affectation of T_{st} and T_{mst}, obtained only as a Si effect. Factors of the cumulative effects of the base and minor elements, used to offer useful information such as on pearlite promoting (*Px*, Equations (4) and (5)) or on antinodularizing action (*K*, Equations (6) and (7)) (Tables 2 and 3) appear to also offer information on the T_{st} and T_{mst} affectation. Figure 5 shows the effect of *Px* (Figure 5a) and *K* (Figure 5b) on the difference between equilibrium temperatures in a stable system ($\Delta T_{st(S\text{-}K)} = T_{st(S)} - T_{st(K)}$) and a metastable system ($\Delta T_{mst(S\text{-}K)} = T_{mst(S)} - T_{mst(K)}$), calculated in *S* (only Si effect) and *K* (full chemistry effect) series.

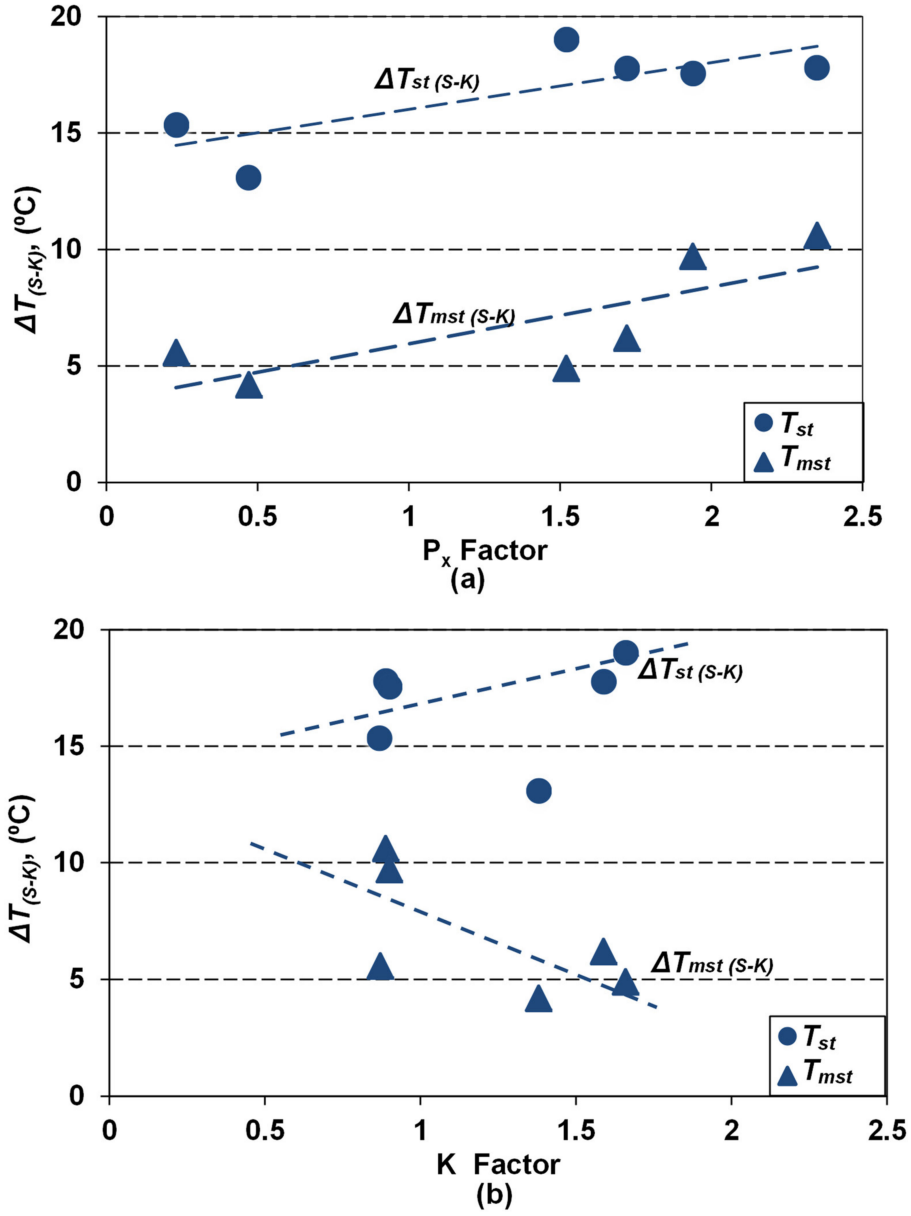

Figure 5. Influence of pearlite promoting factor *Px* (**a**) and antinodularizing factor *K* (**b**) on the difference between equilibrium eutectic temperatures ($\Delta T_{st(S\text{-}K)}$, $\Delta T_{mst(S\text{-}K)}$) calculated only as Si influence (S series) and full chemistry (K series).

Elements promoting pearlite, with a cumulative effect expressed by the *Px* factor, act to increase the difference between both the considered eutectic temperatures ($T_{(S\text{-}K)}$), practically with the same power. The $\Delta T_{(S\text{-}K)}$ factor for high purity cast iron ($Px < 0.5$) reached 4–5 °C for T_{mst} and 13–15 °C for T_{st}, but it will reach 10 °C for T_{mst} and 20 °C for T_{st}, for $Px > 2.0$, respectively.

Elements known with an antinodularizing action, with a cumulative effect expressed by the *K* factor, have different effects on the considered eutectic temperatures (Figure 5b). Factor $\Delta T_{mst(S\text{-}K)}$ decreases (from 5–10 °C up to 4–5 °C) by transition from medium pure cast iron ($K < 1.0$) to lower purity cast iron (K = 1.5–2.0). The $\Delta T_{st(S\text{-}K)}$ factor has an un-conclusive evolution.

Table 5 summarizes the results obtained in thermal (cooling curve) analysis, as selected representative temperatures on the cooling curve, characteristics to the eutectic reaction and the end of solidification, and the undercooling degrees referring to the stable and metastable equilibrium eutectic temperatures, as effects of silicon alloying and inoculation application.

Table 5. Representative parameters of thermal (cooling curve) analysis.

Pr *	Si (%)	Iron	*TEU* (°C)	*TER* (°C)	*TES* (°C)	ΔT_m (°C)	ΔT_1 (°C)	ΔT_2 (°C)	ΔT_3 (°C)	ΔTEU (°C)	ΔTES (°C)
I	2.48	UI ** Inoc ***	1128.4 1142.4	1129.9 1145.1	1050.9 1087.5	23.4 9.4	21.8 35.8	23.3 38.5	−55.7 −19.1	14.0	36.6
II	2.55	UI Inoc	1136.6 1145.8	1136.8 1147.7	1050.4 1097.6	16.8 7.6	28.9 39.1	30.1 41.0	−56.3 −9.1	9.2	47.2
III	3.15	Inoc	1144.53	1156.01	1107.17	16.5	39.52	51.0	2.16		
IV	3.44	UI Inoc	1138.34 1145.97	1141.16 1150.07	1089.03 1098.17	22.37 14.74	38.19 45.82	41.01 49.92	−11.1 −1.98	7.63	9.14
V	4.55	UI Inoc	1156.1 1157.9	1156.6 1158.6	1104.4 1106.7	9.62 7.82	69.89 71.69	70.39 72.39	18.9 20.5	1.8	2.3
VI	5.25	UI Inoc	1156.7 1157.3	1158.9 1158.9	1106.2 1106.5	12.47 11.87	77.59 78.19	79.79 79.79	27.09 27.39	0.6	0.3

* Pr—Experimental Program, ** UI—non-inoculation; *** Inoc—inoculation.

Figure 6 shows the influence of the silicon content and applied inoculation on the representative temperatures characterizing the eutectic formation and the end of solidification, showing: the lowest eutectic reaction temperature (*TEU*), the highest (recalescence) eutectic reaction temperature (*TER*), and the temperature of the end of solidification (*TES*).

Both the silicon content and the inoculation act as favorable influencing factors by increasing all these temperatures, but at different powers depending on the considered temperature and the silicon alloying grade in ductile cast irons, respectively.

Increasing the silicon content from 2.5% up to 5.25% in the present experimental programs leads to increasing the representative temperatures, in both non-inoculated and inoculated ductile cast irons (UI/Inoc): *TEU* (from 1128.4 °C to 1156.7 °C/from 1142.4 to 1157.9°C), *TER* (from 1129.9 °C to 1158.9 °C/from 1145.1 °C to 1158.9 °C) and *TES* (from 1050.4 °C to 1106.2 °C/from 1097.5 °C to 1106.7 °C). The power of increasing the silicon is higher in less than 4.0% Si comparing with the highest silicon content range.

The highest effect of inoculation is visible in non-Si alloyed cast irons (2.5% Si): ΔTEU = 9–14 °C, ΔTER = 11–15 °C and is 3 to 4 four times higher for *TES* (ΔTES = 37–47 °C). For the low level silicon alloying grade (3.15–3.45% Si) beneficial inoculation effect, expressed by temperatures increasing, it is reduced at 7 °C order for *TEU* and *TER* and 9 °C for *TES*, respectively. The highest alloying grade (4.55–5.25% Si) ductile cast irons are characterized by the lowest contribution of inoculation, expressed by ΔTEU = 0.6–1.8 °C, ΔTER = 0–2 °C and ΔTES = 0.3–2.3 °C.

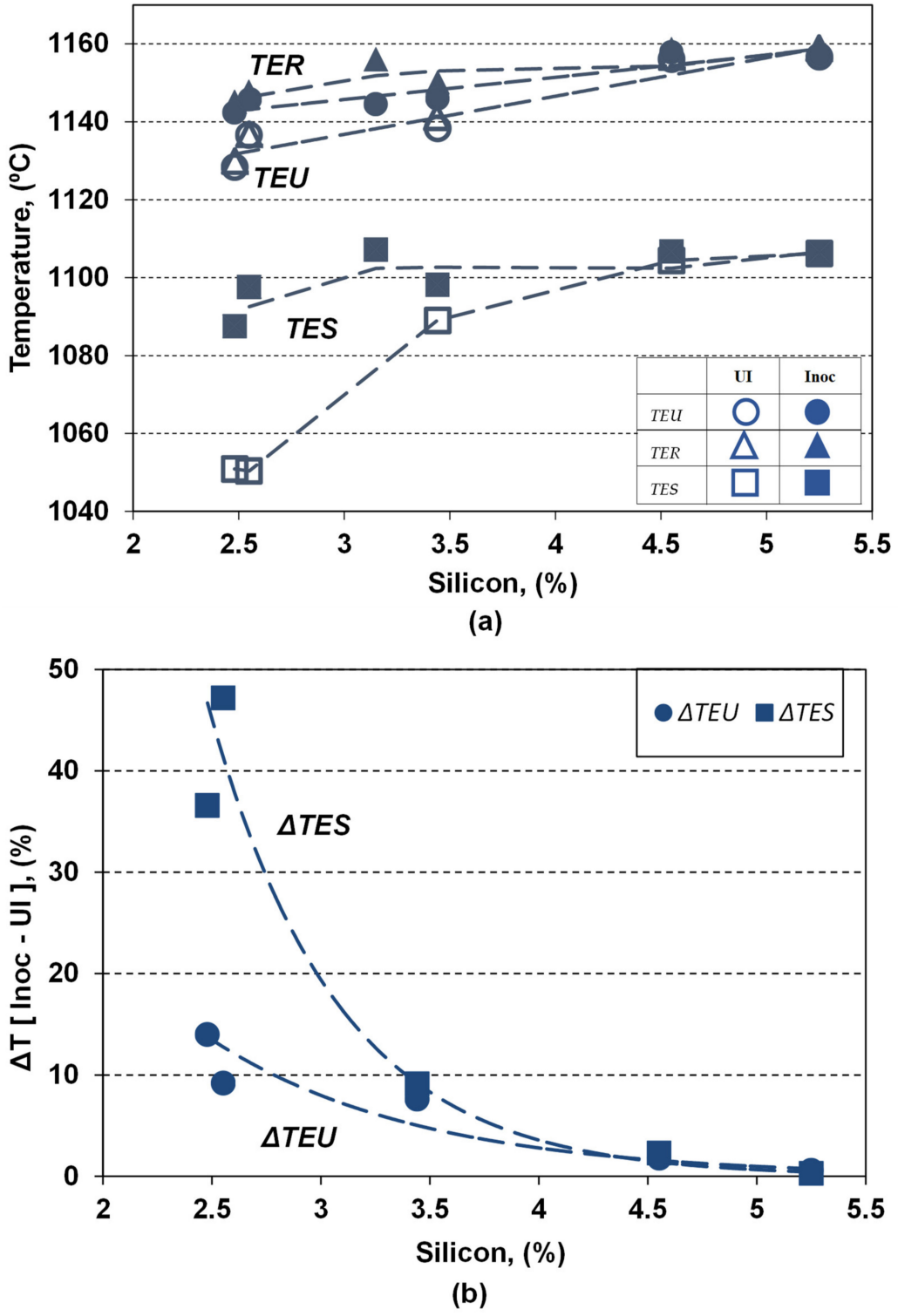

Figure 6. Influence of the silicon content and inoculation on the *TEU*, *TER* and *TES* temperatures (**a**) and the difference between the inoculated and non-inoculated ductile cast irons (Δ*TEU*, Δ*TES*) (**b**).

The representative temperatures *TEU*, *TER* and *TES* could offer useful information especially if they are compared with equilibrium eutectic temperatures, in a stable (graphitic) system T_{st} and in a metastable (carbidic) system T_{mst}. Positions of these temperatures referring to the T_{st}–T_{mst} interval are expressed by a specific undercooling degree.

The most important parameters are illustrated by Equations (8)–(11):

$$\Delta T_{\mathrm{m}} = T_{\mathrm{st}} - TEU \quad (8)$$

$$\Delta T_1 = TEU - T_{\mathrm{mst}} \quad (9)$$

$$\Delta T_2 = TER - T_{\mathrm{mst}} \quad (10)$$

$$\Delta T_3 = TES - T_{\mathrm{mst}} \quad (11)$$

The highest eutectic undercooling ΔT_{m}, as the difference between stable equilibrium eutectic temperature T_{st} and the lowest temperature level on the cooling curve *TEU* offers information on the real undercooling necessary for starting the eutectic reaction. Generally, the higher ΔT_{m} is, the higher is the possibility to form free carbides in the first stage of solidification. But the certitude of the free carbides formation, in specific solidification conditions, could be obtained only if this parameter is higher than the $\Delta T_{\mathrm{s}} = T_{\mathrm{st}}$–$T_{\mathrm{mst}}$ interval.

This means that the eutectic reaction will start below T_{mst} with carbides formation, but without information on the end of the eutectic reaction, when the temperature increased, due to the heat released as solid eutectic formation. Also, no information on it is happened at the end of solidification, in non-equilibrium conditions, specifically for iron castings production in the foundry industry.

Information on these important characteristics of the cast iron solidification could also be obtained by comparing *TEU*, *TER* and *TES* with T_{mst}, resulting in an undercooling degree ΔT_1, ΔT_2 and ΔT_3, respectively. As free carbides could be formed only if the eutectic reaction temperatures are lower than T_{mst}, and graphite is promoted if these temperatures are above T_{mst}, negative values mean carbides and positive values mean graphite, at the beginning of the eutectic reaction (ΔT_1) and at the end of this reaction (ΔT_2), respectively.

Total graphitic structure is illustrated by positive values and total carbidic structure (white cast iron) by negative values, for both ΔT_1 and ΔT_2 parameters. Mottled cast iron is characterized by carbides formation at the beginning of the eutectic reaction (ΔT_1 is negative) and graphite at the end of eutectic reaction (ΔT_2 is positive). The sensitiveness of iron castings to form undesirable defects at the end of solidification, such as free carbides and micro-shrinkage in the areas between eutectic cells is expressed by the ΔT_3 undercooling degree: the higher (more negative) is ΔT_3, the higher is the occurrence of these undesirable events.

Figure 7 shows the variation of the representative undercooling degrees, reporting to T_{st} (ΔT_{m}) and T_{mst} (ΔT_1, ΔT_2, ΔT_3) as effect of silicon content and inoculation application. Silicon favors the increasing of T_{st} and decreasing of T_{mst} ($\Delta T_{\mathrm{s}} = T_{\mathrm{st}}$–$T_{mst}$ enlargement) (Figure 4), and, at the same time, the increasing of *TEU*, *TER* and *TES* parameters (Figure 6). As a result, the undercooling behavior during solidification will be influenced by both of these effects. T_{st} and T_{mst} are considered to be the effects of all the identified elements in the final chemical composition of tested ductile cast irons (K series), including not only silicon influence, but also the complex behavior of the other elements (Figure 2).

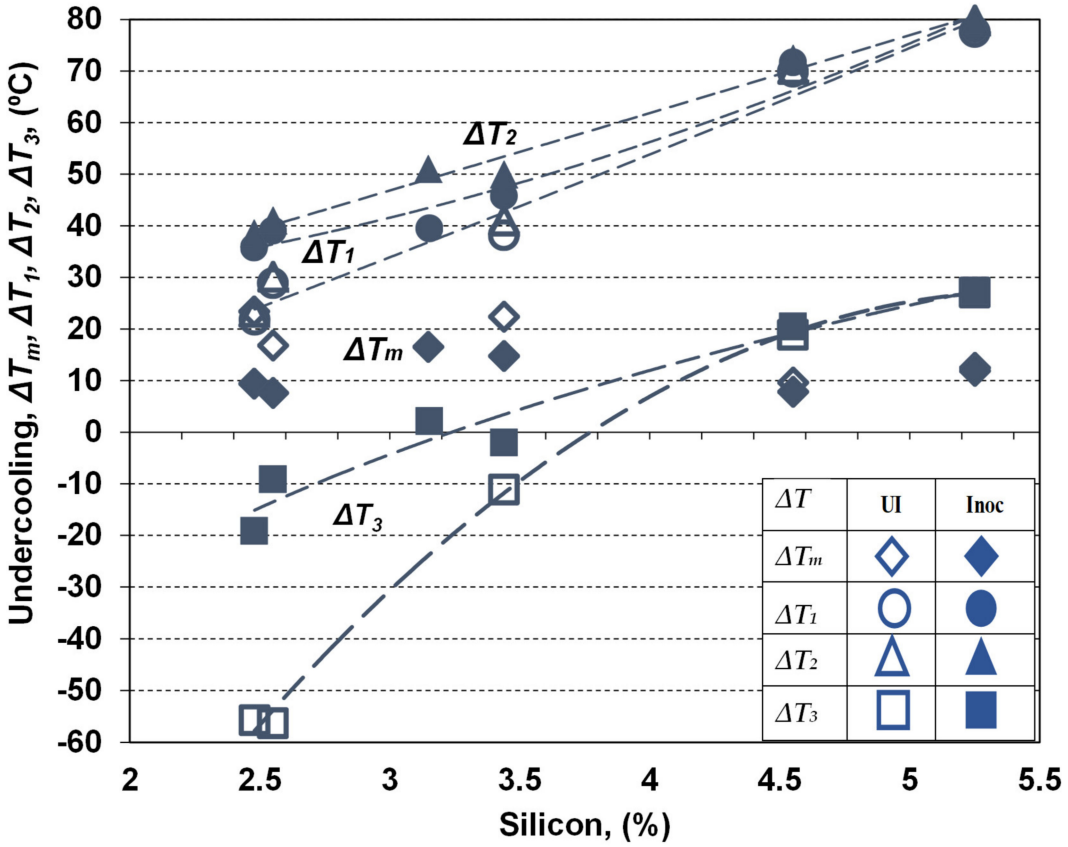

Figure 7. The variation of representative undercooling degrees, reporting to T_{st} (ΔT_m) and T_{mst} (ΔT_1, ΔT_2, ΔT_3) as the effect of silicon content and inoculation application.

Generally, silicon contributes to ΔT_m decreasing and ΔT_1, ΔT_2 and ΔT_3 (less negative) increasing, with supplementary positive contribution of inoculation in the same direction. The highest undercooling degrees characterize the non-Si alloyed ductile cast irons (2.5% Si), while the silicon alloying leads to decreasing the undercooling degrees, on the entire solidification time, but in a different way for eutectic reaction and at the end of solidification, and for non-inoculated and inoculated Mg-treated cast irons, respectively.

The lower limit of Si-alloyed cast irons (3.15–3.45% Si) are characterized by 1.4–1.6 times higher eutectic undercooling, with 2–3 times beneficial effects for the higher silicon level (4.55–5.25% Si). The positive effect of silicon alloying is higher for non-inoculated cast irons, and especially at the end of solidification.

Inoculation has an important contribution to reduce the undercooling degree; ΔT_m reached a lower level and ΔT_1, ΔT_2 and ΔT_3 reached a higher level, respectively. From this point of view, this metallurgical treatment is very important for the non-Si alloyed ductile cast irons; it is visible for less than 3.5% Si (medium range), but with only a small contribution for more than 4.5% Si.

A special remark for the undercooling at the end of solidification (ΔT_3): it becomes positive for more than 4% Si non-inoculated and 3.2% Si inoculated ductile cast irons.

The cumulative effects of silicon alloying and inoculation could also be expressed by the ratio between the highest eutectic undercooling reporting to the stable eutectic temperature (ΔT_m) and the eutectic interval in stable and metastable systems, $\Delta T_s = T_{st} - T_{mst}$ (Figure 8). This ratio is at the 0.4–0.5 level for non-inoculated and 0.15–0.20 for inoculated, 2.5% Si ductile cast irons, but it is decreased up to 0.12–0.14 and 0.10–0.13, respectively, for the highest silicon content.

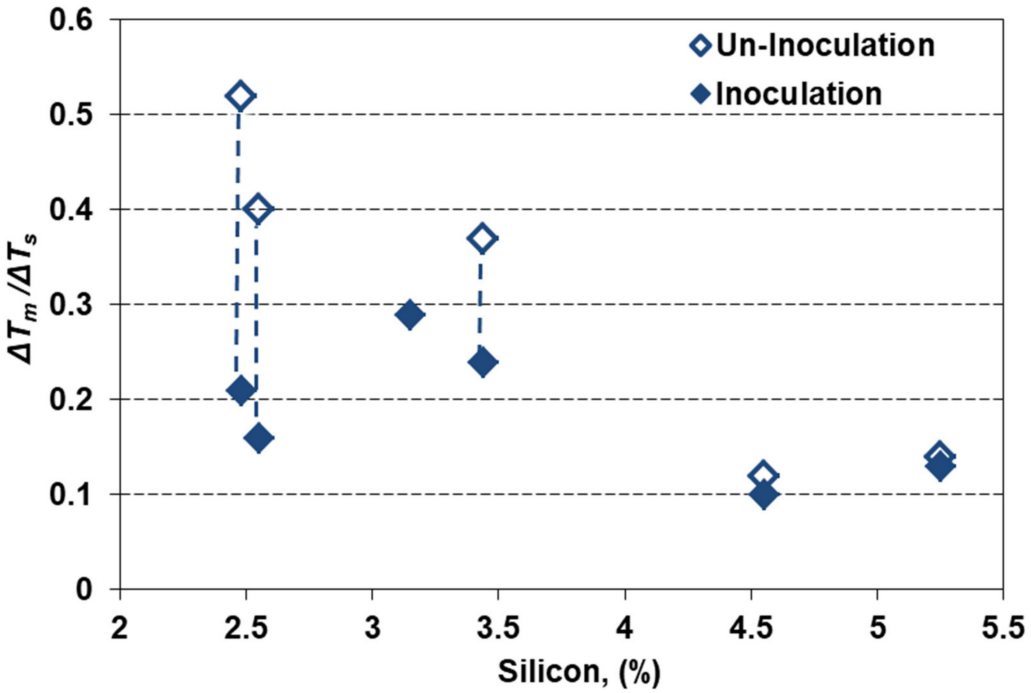

Figure 8. The cumulative effects of silicon alloying and inoculation on the eutectic undercooling level.

Generally, the $\Delta T_m/\Delta T_s$ ratio is strongly affected by inoculation for less than 3.5% Si, but at a lower level, and less affected by inoculation for more than 4.5% Si. The 2.5–3.5% Si ductile cast irons are more sensitive to high solidification undercooling (but with a higher efficiency of inoculation), comparing to 4.5–5.5% Si cast irons, at a lower undercooling level (but also at a lower inoculation effect). In high Si-ductile cast irons (especially for more than 4% Si) the main objective of inoculation is not carbides avoiding, but the improvement of the nodular graphite compactness degree (affected by Si) [2,11,20].

It was found that the solidification time has a significant effect on the microstructure and mechanical properties of solution strengthened ferritic ductile iron. In particular, it has been found that with increasing solidification times, the microstructure becomes coarser and the presence of defects increases. Moreover, the lower the cooling rate, the lower the measured tensile and fatigue properties [21]. A recent work [22] found that the melt quality is closely associated with the resultant morphology and number of austenite dendrites, graphite nodules, and matrix structure, in thin-walled ductile iron castings.

4. Conclusions

The present paper evaluates by a thermal (cooling curve) analysis the solidification pattern of ductile cast irons, non-Si alloyed (<3.0% Si), low (3.0–3.5% Si) and medium Si alloyed (4.5–5.5% Si), as silicon content increases and inoculation is applied with simultaneous effects. The following conclusions could be drawn.

- Chemical analysis focuses not only on the base elements but also on the minor elements, such as their cumulative effects such as the pearlite formation sensitiveness, antinodularizing action and on the values of eutectic temperatures in stable (graphitic) and metastable (carbidic) Fe-C-Si-*Xi* systems.
- Silicon is an important influencing factor, but the base and minor elements affect the equilibrium eutectic temperatures, inclusively at high Si-content, much more in the Fe-C-Si-*Xi* stable system (ΔT_{st} = 15–20 °C) than in the metastable system (ΔT_{mst} = 5–10 °C), comparing their calculations with only the Si effect (Fe-C-Si system), where the highest values resulted.
- It is found that higher is the pearlite formation potential (*Px*), the higher is the affectation of T_{st} and T_{mst}, obtained only as a Si effect: from 4–5 °C for T_{mst} and 13–15 °C

for T_{st} in high purity cast iron ($Px < 0.5$) up to 10 °C for T_{mst} and 20 °C for T_{st}, for $Px > 2.0$.

- Elements known to have an antinodularizing action, with cumulative effect expressed by K factor, decrease T_{mst} (from 5–10 °C up to 4–5 °C) by transition from a medium pure cast iron ($K < 1.0$) to a lower purity cast iron ($K = 1.5$–2.0), without a conclusive evolution for T_{st}.
- Both Si-content and inoculation act as favorable influencing factors, by increasing the representative temperatures and decreasing the undercooling degrees for the eutectic reaction and at the end of solidification, but at a different power depending on the considered temperature and the Si-alloying grade.
- The highest positive effect of inoculation is visible in non-Si alloyed cast irons (2.5% Si): 9–15 °C for the eutectic reaction and 3 to 4 times increased at the end of solidification (37–47 °C). Increased Si content decreases the inoculation power to 7–9 °C for a low alloying grade (up to 3.5% Si), with the lowest contribution at more than 4.5% Si (0.3–2.0 °C).
- Si favors increasing of the eutectic interval (T_{st}–T_{mst}), and, at the same time, the increasing of temperatures for the eutectic reaction and, at the end of solidification, with other elements contribution, as well. As a result, the undercooling behavior during solidification will be influenced by both effects.
- The highest undercooling characterizes the non-Si alloyed cast irons, while the lower limit of Si-alloyed cast irons are characterized by 1.4–1.6 times lower eutectic undercooling, with 2–3 times higher beneficial effect for the higher Si level. The positive effect of Si-alloying is higher for non-inoculated cast irons, and especially at the end of solidification.
- Inoculation has an important contribution to reduce the undercooling degree, being very important for the non-Si alloying, visible for less than 3.5% Si, but with only a small contribution for more than 4.5% Si. A special remark for the undercooling at the end of solidification, which becomes positive for more than 4% Si non-inoculated and 3.2% Si inoculated ductile cast irons.
- 2.5–3.5% Si ductile cast irons are more sensitive to high solidification undercooling (but with a higher efficiency of inoculation), comparing to 4.5–5.5% Si cast irons, at a lower undercooling level (but also at a lower inoculation effect). In high Si-ductile cast irons (especially for more than 4% Si) the main objective of inoculation is not carbides avoiding, but the improvement of the nodular graphite compactness degree (affected by Si). This could be important especially in the furan resin molding technique, where Sulphur in P-toluenesulphonic acid (PTSA), usually is used as the hardener, has been identified as an important factor causing graphite degeneration [23].

Author Contributions: I.S., D.A., S.S. and I.R. contributed equally in conceiving, designing and performing the experiments; analyzing the data; and writing the paper. All authors have read and agreed to the published version of the manuscript.

Funding: This research received no external funding.

Data Availability Statement: Not applicable.

Conflicts of Interest: The authors declare no conflict of interest.

References

1. Stets, W.; Loblich, H.; Gassner, G.; Schumacher, P. Solution Strengthened Ferritic Ductile Cast Iron According DIN EN1563:2012–Properties, Production and Application. In Proceedings of the "Keith Millis" Symposium on Ductile Iron, Nashville, TN, USA, 15–17 October 2013; pp. 283–292.
2. Stan, S.; Riposan, I.; Chisamera, M.; Barstow, M. Solidification Pattern of Silicon Alloyed Ductile Cast Irons. In Proceedings of the 122nd AFS Metalcasting Congress, Fort Worth, TX, USA, 3–5 April 2018; pp. 18–22.
3. EN 1563 Founding—Spheroidal Graphite Cast Irons. Available online: https://www.en-standard.eu/csn-en-1563-founding-spheroidal-graphite-cast-irons/ (accessed on 13 March 2021).

4. Automotive Ductile Iron Castings for High Temperature Applications J2582_200406. Available online: https://www.sae.org/standards/content/j2582_200406/ (accessed on 13 March 2021).
5. Riposan, I.; Skaland, T. Modification and Inoculation of Cast Iron. In *Cast Iron Science and Technology Handbook*; Stefanescu, D.M., Ed.; American Society of Materials: Materials Park, OH, USA, 2017; pp. 160–176.
6. Stefanescu, D.M. Thermal Analysis-Theory and Applications in Metalcasting. *Int. J. Metalcasting* **2015**, *9*, 7–22. [CrossRef]
7. Sparkman, D. Microstructure by Thermal Analysis. *AFS Trans.* **2011**, *119*, 413–419.
8. Cojocaru, A.M.; Riposan, I.; Stan, S. Solidification Influence in the Control of Inoculation Effects in Ductile Cast Irons by Thermal Analysis. *J. Therm. Anal. Calorim.* **2019**, *138*, 2131–2143. [CrossRef]
9. Anca, D.; Chisamera, M.; Stan, S.; Stan, I.; Riposan, I. Sulfur and Oxygen Effects on High-Si Ductile Iron Casting Skin Formation. *Coatings* **2020**, *10*, 618. [CrossRef]
10. Anca, D.; Chisamera, M.; Stan, S.; Riposan, I. Graphite Degeneration in High Si, Mg-Treated Iron Castings—Sulfur and Oxygen Addition Effects. *Int. J. Met.* **2019**, *14*, 663–671. [CrossRef]
11. Riposan, I.; Stefan, E.; Stan, S.; Pana, N.R.; Chisamera, M. Effects of Inoculation on Structure Characteristics of High Silicon Ductile Cast Irons in Thin Wall Castings. *Metals* **2020**, *10*, 1091. [CrossRef]
12. QuiK-Cup®QuiK-Lab®E Thermal Analysis of Cast Iron. Available online: https://www.heraeus.com/media/media/hen/media_hen/products_hen/iron/QuikLabE_QuikCup_EN_lowres.pdf (accessed on 13 March 2021).
13. Thielemann, T. Zur Wirkung van Spurenelementen in Gusseisen mit Kugelgraphit [Effects of trace elements in nodular graphite cast irons]. *Giessereitechnik* **1970**, *16*, 16–24.
14. Dommaaschk, C. Chances and Limits of High Silicon Ductile Iron. In Proceedings of the WFO Technical Forum, Gauteng, Africa, 14–17 March 2017.
15. Hammersberg, P.; Hamberg, K.; Bjorkegren, L.E.; Lindkvist, J.; Borgstrom, H. Sensitivity to Variation of Tensile Properties of High Silicon Ductile Iron. *Mater. Sci. Forum* **2018**, *925*, 280–287. [CrossRef]
16. Zhou, J. Colour Metallurgy of Cast Iron. *China Foundry* **2009**, *6*, 57–69.
17. Sillen, R.V. Novacast Technologies. 2006. Available online: www.novacast.se (accessed on 10 December 2006).
18. Kanno, T.; Iwami, Y.; Kang, I. Prediction of Graphite Nodule Count and Shrinkage Tendency in Ductile Cast Iron With 1 Cup Thermal Analysis. *Int. J. Metalcast.* **2017**, *11*, 94–100. [CrossRef]
19. Kanno, T.; Fukuda, Y.; Morinaka, M.; Nakae, H. Effect of Alloying Elements on Graphite and Cementite Eutectic Temperature of Cast Iron. *J. JFS.* **1998**, *70*, 465–470.
20. Stan, S.; Riposan, I.; Chisamera, M.; Stan, I. Solidification Characteristics of Silicon Alloyed Ductile Cast Irons. *J. Mater. Eng. Perform.* **2019**, *28*, 278–286. [CrossRef]
21. Borsato, T.; Ferro, P.; Berto, F.; Carollo, C. Effect of Solidification Time on Microstructural, Mechanical and Fatigue Properties of Solution Strengthened Ferritic Ductile Iron. *Metals* **2019**, *9*, 24. [CrossRef]
22. Gorny, M.; Kawalec, M.; Sikora, G.; Olejnik, E.; Lopez, H. Primary Structure and Graphite nodules in Thin-Walled High-Nickel Ductile Iron Castings. *Metals* **2018**, *8*, 649. [CrossRef]
23. Ivan, N.; Chisamera, M.; Riposan, I. Graphite Degeneration In the Surface Layer of Ductile Iron Castings. *Int. J. Cast Met. Res.* **2013**, *26*, 138–142. [CrossRef]